Chapter 9
Compensation of Rate-Dependent Hysteresis in a Piezomicropositioning Actuator

Mohammad Al Janaideh

Abstract Piezomicropositioning actuators exhibit strong rate-dependent hysteresis nonlinearities that affect the accuracy of these micropositioning systems in open-loop system and may even lead to system instability of the closed-loop control system. Compensation of rate-dependent hysteresis effects using inverse rate-independent hysteresis models may yield high compensation error at high-excitation frequencies since these hysteresis effects increase as the excitation frequency of the input voltage increases. The inverse rate-dependent Prandtl–Ishlinskii model is utilized for compensation of the rate-dependent hysteresis nonlinearities in a piezomicropositioning stage. The exact inversion of the rate-dependent model is on hold under the condition that the distances between the thresholds do not decrease in time. The inverse of the rate-dependent model is applied as a feedforward compensator to compensate for the rate-dependent hysteresis nonlinearities of a piezomicropositioning actuator at different excitation frequencies between 0.1 and 50 Hz. The results show that the inverse compensator suppresses the hysteresis percent and the maximum positioning error in the output displacement of the piezomicropositioning actuator at different excitation frequencies, respectively.

9.1 Introduction

Piezomicropositioning actuators are increasingly used in micro and nano-positioning applications because of their advantages which include nanometer resolution, high stiffness, and fast response [1–9]. However, piezomicropositioning

M. Al Janaideh (✉)
Department of Mechatronics Engineering, The University of Jordan, Amman 11942, Jordan

Department of Aerospace Engineering, The University of Michigan, Ann Arbor, MI 48109, USA
e-mail: aljanaideh@gmail.com

M. Rakotondrabe (ed.), *Smart Materials-Based Actuators at the Micro/Nano-Scale: Characterization, Control, and Applications*, DOI 10.1007/978-1-4614-6684-0_9,

actuators show hysteresis nonlinearities between the applied input voltage and output displacement. These nonlinearities have been associated with oscillations in the open-loop system's responses, and poor tracking performance and potential instabilities of the closed-loop system [10]. Different piezomicropositioning actuators show obvious increase in hysteresis nonlinearities when the excitation frequency of the applied input voltage increases in a nonlinear manner [11–15]. The inverse-based control methods generally employ a cascade of a rate-independent hysteresis model and its inverse together with a controller to compensate for the error of the compensation in piezomicropositioning actuators; see for example [16]. These methods, however, necessitate the formulation of the hysteresis model inverse, which is often a challenging task.

Different closed-loop control systems, however, have been proposed with inverse rate-independent hysteresis models to compensate for hysteresis nonlinearities at different excitation frequencies. Ge and Jouaneh [16] used inverse Preisach model, which was obtained using a numerical algorithm, as a feedforward compensator with PID feedback control system. Hu et al. [17] applied inverse Preisach model formulated with a dynamic density function in a closed-loop control system. In a similar manner, Song et al. [18] applied the inverse Preisach model with PD-lag and PD-lead controllers in a closed-loop control system. Esbrook et al. [19] applied a servocompensator with inverse Prandtl–Ishlinskii model in a closed-loop control system. Shan and Leang[20] applied discrete-time repetitive controller combined with an inverse hysteresis compensator based on the Prandtl–Ishlinskii model. Feedback control techniques could compensate for the rate-dependent hysteresis in peizomicropositioning actuators. However, the accurate and large bandwidth sensors as well as the feedback control techniques inserted in the closed-loop control systems may limit the use of the piezomicropositioning systems in different industrial applications. Ang et al. [21] applied the inverse modified Prandtl–Ishlinskii model as a feedforward compensator to compensate for hysteresis nonlinearities under different excitation frequencies.

In this chapter, the open-loop control technique is applied to compensate for the rate-dependent hysteresis nonlinearities over different excitation frequencies. The rate-dependent hysteresis nonlinearities are characterized using the rate-dependent Prandtl–Ishlinskii model. The analytical exact inverse of the rate-dependent Prandtl–Ishlinskii model is formulated and applied as a feedforward compensator to compensate for the rate-dependent hysteresis nonlinearities in a piezomicropositioning actuator. The main advantage of the rate-dependent Prandtl–Ishlinskii model over the other hysteresis models used in the literature is that its inverse can be attained analytically, and it can be implemented as a feedforward compensator to control the piezomicropositioning actuator over different excitation frequencies without inserting feedback control techniques.

In [7, 22], the analytical inverse of the Prandtl–Ishlinskii model is constructed with dynamic thresholds. The explicit inversion formula for the Prandtl–Ishlinskii model presented in [23] remains applicable also for the case of time-dependent thresholds, provided the distances between them do not decrease in time. This

inverse is applied in this chapter as a feedforward controller in order to compensate for the rate-dependent hysteresis nonlinearities. Such compensations are experimentally illustrated by a piezomicropositioning actuator.

9.2 Background

The Prandtl–Ishlinskii model integrates play operators Γ_r with different thresholds r and with positive weights in order to characterize hysteresis nonlinearities in actuators and materials; see [23, 24]. For $t \in [0,T]$, when an input $u(t) \in C[0,T]$ is applied, where $C[0,T]$ is the space of continuous functions on the time interval $[0,T]$, the output of the Prandtl–Ishlinskii model for $i = 1,\ldots,n$, where n is an integer represents the number of the play operators, is given, according to [23], by the formula

$$\Pi[u](t) = a_0 u(t) + \sum_{i=1}^{n} a_i \Gamma_{r_i}[u,x_i](t), \tag{9.1}$$

where a_0 and a_i are positive weights.

The Prandtl–Ishlinskii model (9.1) is a rate-independent hysteresis model, attributed to the time-independent play operator that the model employs. This model has a unique advantage since it admits an exact inverse, which has been established in [25]. In [23], the output of the inverse rate-independent independent Prandtl–Ishlinskii model is written in the form

$$\Pi^{-1}[u](t) = b_0 u(t) + \sum_{i=1}^{n} b_i \Gamma_{s_i}[u,y_i](t). \tag{9.2}$$

This inverse has been widely applied as a feedforward controller to compensate for hysteresis nonlinearities in smart-material actuators at low-excitation frequencies of the applied input. However, these actuators exhibit hysteresis nonlinearities that are strongly rate-dependent. Consequently, the use of the inverse rate-independent Prandtl–Ishlinskii model as a feedforward compensator may cause considerable errors in the output displacement. It is therefore necessary to design a model and a compensator capable of incorporating rate-dependent hysteresis effects. This can be accomplished by adding a viscosity term in the constitutive relation [7].

9.3 Rate-Dependent Prandtl–Ishlinskii Model and Its Inverse

In this section the rate-dependent Prandtl–Ishlinskii model and its inverse are presented. The rate-dependent Prandtl–Ishlinskii model is employed in this study to characterize the rate-dependent hysteresis nonlinearities in a piezomicropositioning

stage. This model is formulated in [22] using a play operator of time-dependent (dynamic) threshold.

9.3.1 The Rate-Dependent Prandtl–Ishlinskii Model

Let $AC(0,T)$ the space of real absolutely continuous functions defined on the interval $[0,T]$. For an input $u(t) \in AC(0,T)$, the output of the rate-dependent Prandtl–Ishlinskii model, constructed based on the rate of the applied input $\dot{u}(t)$, is given by the formula

$$\Psi[u](t) = a_0 u(t) + \sum_{i=1}^{n} a_i \Phi_{r_i(\dot{u}(t))}[u, x_i](t). \tag{9.3}$$

The output of the rate-dependent play operator is denoted as

$$z_i(t) = \Phi_{r_i(\dot{u}(t))}[u, x_i](t). \tag{9.4}$$

Let x_i be given initial conditions for $i = 1, 2, \ldots, n$ such that for $i = 1, \ldots, n-1$

$$\begin{aligned} |x_1| &\leq r_1(\dot{u}(0)), \\ |x_{i+1} - x_i| &\leq r_{i+1}(\dot{u}(0)) - r_i(\dot{u}(0)). \end{aligned} \tag{9.5}$$

The dynamic thresholds $r_i(t)$ are defined for $t \in [0,T]$ as

$$0 \leq r_1(\dot{u}(t)) \leq r_2(\dot{u}(t)) \leq \cdots \leq r_n(\dot{u}(t)). \tag{9.6}$$

As shown in [11], the rate-dependent Prandtl–Ishlinskii model can characterize the rate-dependent hysteresis nonlinearities in piezomicropositioning actuators over different excitation frequencies. The inverse of the rate-dependent Prandtl–Ishlinskii model is achievable and can be applied as a feedforward compensator to compensate for the rate-dependent hysteresis nonlinearities in real-time systems.

9.3.2 Inverse Rate-Dependent Prandtl–Ishlinskii Model

The concept of the open-loop control system is used to obtain identity mapping between the input $u(t)$ and the output $v(t)$ such that $u(t) = v(t)$. When the output of the exact inverse of the rate-dependent Prandtl–Ishlinskii model $\Psi^{-1}[u](t)$ is applied as a feedforward controller to compensate for the rate-dependent hysteresis

nonlinearities presented by the rate-dependent Prandtl–Ishlinskii model $\Psi[u](t)$, the output of the compensation is expressed as

$$v(t) = \Psi \circ \Psi^{-1}[u](t). \tag{9.7}$$

The exact inversion is on hold under the condition that the distances between the dynamic thresholds $r_i(\dot{u}(t))$ do not decrease in time [22]. Analytically for $\forall i = 1, \ldots, n-1$

$$\frac{\mathrm{d}}{\mathrm{d}t}\left(r_{i+1}(\dot{u}(t)) - r_i(\dot{u}(t))\right) \geq 0. \tag{9.8}$$

The proof of the inversion formula is based in a substantial way on the so-called Brokate formula for the superposition of play operators with different thresholds. It was established for constant thresholds in [26], and the extension to moving thresholds has been done in [22]. The inverse of the rate-dependent Prandtl–Ishlinskii is also a rate-dependent Prandtl–Ishlinskii model. The output of the inverse model is expressed as

$$\Psi^{-1}[u](t) = b_0, u(t) + \sum_{i=1}^{n} b_i \Phi_{s_i(\dot{u}(t))}[u, y_i](t). \tag{9.9}$$

Let the output of the rate-dependent play operator of the inverse model is

$$d_i(t) = \Phi_{s_i(\dot{u}(t))}[u, y_i](t). \tag{9.10}$$

The thresholds of the inverse model are

$$\begin{aligned} s_1(\dot{u}(t)) &= a_0 r_1(\dot{u}(t)), \\ s_{i+1}(\dot{u}(t)) - s_i(\dot{u}(t)) &= \left(\sum_{j=0}^{i} a_j\right)\left(r_{i+1}(\dot{u}(t)) - r_i(\dot{u}(t))\right). \end{aligned} \tag{9.11}$$

The weights of the inverse model $b_0, b_1, \ldots, b_n$ are

$$\begin{aligned} b_0 &= \frac{1}{a_0}, \\ b_i &= \frac{1}{\sum_{j=0}^{i} a_j} - \frac{1}{\sum_{j=0}^{i-1} a_j}. \end{aligned} \tag{9.12}$$

The initial conditions of the inverse model $y_1, y_2, \ldots, y_n$ are

$$\begin{aligned} y_1 &= a_1 x_1, \\ y_{i+1} - y_i &= \left(\sum_{j=0}^{i} a_j\right)(x_{i+1} - x_i). \end{aligned} \tag{9.13}$$

9.3.3 The Dynamic Threshold

The following dynamic thresholds are used:

$$r_i(\dot{u}(t)) = \alpha_i + g(\dot{u}(t)). \tag{9.14}$$

This can be shown to be mathematically equivalent to modeling hysteresis and creep by means of an analogical model with elastic, plastic, and viscous elements as in [7,27]. Then

$$\alpha_i - \alpha_{i-1} \geq \sigma, \tag{9.15}$$

where σ is a positive constant. The constants α_i in (9.14) represent the rate-independent hysteresis effects, while the function $g(\dot{u}(t))$ is proposed to characterize the rate-dependent hysteresis effects. With this choice

$$r_{i+1}(\dot{u}(t)) - r_i(\dot{u}(t)) \geq 0 \tag{9.16}$$

and

$$\frac{\mathrm{d}}{\mathrm{d}t}\left(r_{i+1}(\dot{u}(t)) - r_i(\dot{u}(t))\right) = 0. \tag{9.17}$$

From these equations it can be concluded that the exact inversion formula for the rate-dependent Prandtl–Ishlinskii model holds. It should be mentioned that the proposed formulation for the dynamic threshold reduces the rate-dependent Prandtl–Ishlinskii model $\Psi[u](t)$ into the rate-independent Prandtl–Ishlinskii model $\Pi[u](t)$ for $g(\dot{u}(t)) = 0$.

9.3.4 Numerical Implementation

The numerical implementation of the rate-dependent Prandtl–Ishlinskii model and its inverse is presented for an input $u(t)$ with h sampling time. The rate of the applied input $\dot{u}(t)$ can be estimated for $k = 1, 2, 3, \ldots, K = T/h$ as

$$u_s(k) = \frac{u(k) - u(k-1)}{h}, \tag{9.18}$$

where

$$h = t(k) - t(k-1). \tag{9.19}$$

The discrete dynamic threshold is presented as

$$r_i(u_s(k)) = \alpha_i + g(u_s(k)). \tag{9.20}$$

The discrete output of the rate-dependent play operator is expressed as

$$z_i(k) = \max(u(k) - r_i(u_s(k)), \min(u(k) + r_i(u_s(k)), z_i(k-1))). \tag{9.21}$$

The discrete output of rate-dependent Prandtl–Ishlinskii model can thus be derived as

$$\Psi[u](k) = a_0 u(k) + \sum_{i=1}^{n} a_i \Phi_{r_i(u_s(k))}[u](k). \tag{9.22}$$

The discrete output of the inverse rate-dependent Prandtl–Ishlinskii model can thus be expressed as

$$\Psi^{-1}[u](k) = b_0 u(k) + \sum_{i=1}^{n} b_i \Phi_{s_i(u_s(k))}[u](k). \tag{9.23}$$

9.4 Experimental Results and Hysteresis Modeling

9.4.1 Experimental Results

The experiments were performed on a piezomicropositioning actuator (P-753.31C) from Physik Instrumente Company. The actuator provided maximum displacement of 100 µm from its static equilibrium position, and it integrates a capacitive sensor (sensitivity = 1 µm/V; resolution 0.1 nm) for measurement of stage displacement response. The excitation module compromises a voltage amplifier (LVPZT, E-505) with a fixed gain of 10, which provides the excitation voltage to the actuator. The actuator displacement response signal was acquired by a DSpace DS1104 controller board. The measurements with the piezomicropositioning stage were performed under a harmonic input of $u(t) = 40\cos(2f\ \pi\ t)$ at seven excitation frequencies (1, 5, 10, 20, 30, 40, and 50 Hz). The input voltage and output displacement signals were acquired at a sampling frequency of 10 KHz.

The measured data were further analyzed to quantify hysteresis and displacement attenuation as a function of the applied excitation frequency. The resulting hysteresis loops relating displacement responses to the input voltage are shown at excitation frequencies in Fig. 9.1. The results show that hysteresis nonlinearities increase with increasing the excitation frequency of the applied input voltage. It is evident that the micropositioning stage exhibits highly rate-dependent hysteresis effects between the input voltage and the output displacement.

9.4.2 Parameter Identification

Parameter identifications of the rate-dependent Prandtl–Ishlinskii model are presented in this section. Measured rate-dependent hysteresis loops between the applied input voltage and the output displacement are used to identify the parameters of the rate-dependent Prandtl–Ishlinskii model and its inverse. Let $g(\dot{u}(t)) = \beta(\dot{u}(t))^2$.

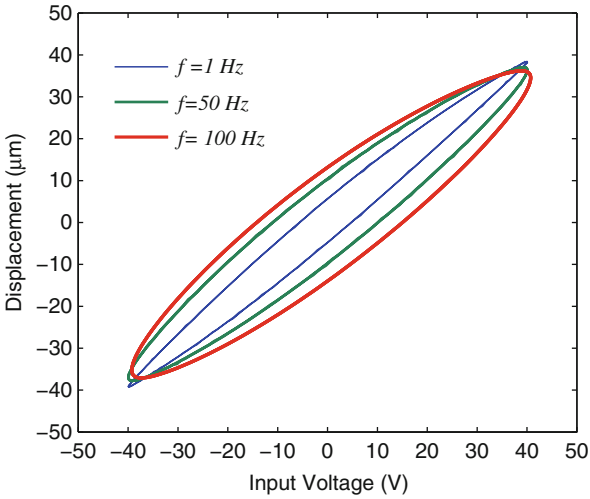

Fig. 9.1 Hysteresis loops at different excitation frequencies

The parameter vector $X = \{\beta, \zeta, a_0, a_1, a_2, \ldots, a_n\}$ was identified through minimization of the an error function over different excitation frequencies. This function is given by

$$Q(X) = \Theta(k). \tag{9.24}$$

The model error function Θ is used to identify the parameters of the rate-dependent Prandtl–Ishlinskii model $\Psi[v](t)$. The error function Θ is expressed as

$$\Theta(k) = \sum_{p=1}^{P} \sum_{k=1}^{K} A_p (\Psi[v](k) - y_m(k))^2, \tag{9.25}$$

where $\Psi[v](k)$ is the displacement response of the model corresponding to a particular excitation frequency and $y_m(k)$ is the measured displacement under the same excitation frequency. The model error function is constructed through summation of squared errors over a range of input frequencies, denoted by p ($p = 1, 2, \ldots, P$). The index k ($k = 1, \ldots, K$) refers to the number of data points considered to compute the error function Q for one complete hysteresis loop. Two hundred data points ($K = 200$) were available for each measured hysteresis loop. Seven excitation frequencies ($P = 7$) of 1, 5, 10, 20, 30, 40, and 50 Hz are used. Owing to the higher error at excitation frequencies, a weighting constant A_p was introduced to emphasize the error minimization at higher excitation frequencies. The weights A_p for $p = 1, 2, \ldots, 7$ are selected based on the hysteresis percent as

$$A_p = \frac{H_p}{H_1}, \tag{9.26}$$

where H_p represents the hysteresis percent for the p excitation frequency. The weights A_p are obtained as: 1, 1.18, 1.38, 1.57, 1.78, and 1.96 for 1, 5, 10, 20, 30, 40,

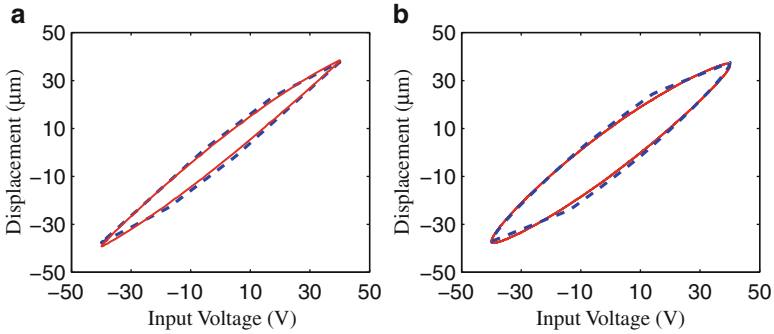

Fig. 9.2 Comparison between the output of the rate-dependent Prandtl–Ishlinskii model (*solid line*) and the measured hysteresis nonlinearities (*dashed line*) in the piezomicropositioning actuator at: (**a**) 1 Hz and (**b**) 50 Hz

and 50 Hz, respectively. The error minimization is performed using the MATLAB constrained optimization toolbox subject to the following constraints:

$$(\beta, \zeta, a_0, a_1, a_2) > 0, \zeta \gg \beta. \tag{9.27}$$

The rate-dependent Prandtl–Ishlinskii model is used to characterize the rate-dependent hysteresis nonlinearities of the piezomicropositioning actuator between 1 and 50 Hz. The results propose two rate-dependent play hysteresis operators $(n = 2)$ to characterize the rate-dependent hysteresis nonlinearities.

9.4.3 Hysteresis Modeling

The validity of the model was examined by comparing the model displacement responses to the measured data. The results suggest that the model can effectively predict the hysteresis properties of the piezomicropositioning actuator at different excitation frequencies between 1 and 50 Hz. Figure 9.2 shows the capability of the model to characterize the rate-dependent hysteresis nonlinearities at 1 and 50 Hz.

9.5 Feedforward Compensation of Rate-Dependent and Rate-Independent Hysteresis Nonlinearities

In this section the inverse rate-dependent Prandtl–Ishlinskii model is applied as a feedforward compensator to compensate for hysteresis nonlinearities under different excitation frequencies.

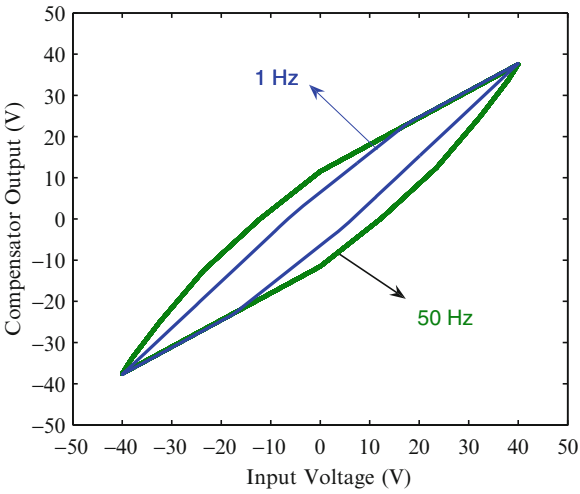

Fig. 9.3 The input–output characteristics of the inverse rate-dependent Prandtl–Ishlinskii model at excitation frequencies of 1 and 50 Hz

9.5.1 The Inverse Compensator

The input–output characteristics of the inverse rate-dependent Prandtl–Ishlinskii model at excitation frequencies of 1, 20, and 50 Hz are shown in Fig. 9.3. This figure shows that hysteresis nonlinearities in the output of the inverse model increase as the excitation frequency of the input voltage increases.

9.5.2 Compensation of Rate-Dependent Hysteresis

The inverse rate-dependent Prandtl–Ishlinskii model obtained in the previous section is applied as a feedforward compensator to compensate for the rate-dependent hysteresis nonlinearities between 1 and 50 Hz. The measured output–input characteristics of the piezomicropositioning stage with inverse compensator are illustrated in Fig. 9.4 at excitation frequencies of 1, 20, and 50 Hz. The results show that the inverse rate-dependent model can effectively compensate the hysteresis effects at different excitation frequencies. Figure 9.5 shows the time history of the input voltage and the measured displacement with and without the inverse compensator at excitation frequency of 50 Hz.

The positioning error is computed as the deviation between measured displacement and the input voltage, which represents the desired displacement, at different excitation frequencies (Fig. 9.6). Figure 9.7 illustrates comparison of the maximum positioning errors with and without the inverse compensator. Without the inverse compensator, the maximum positioning errors are between 6.5 and 13.8 µm, while the measured responses with the inverse compensator show maximum positioning errors between 2.3 and 3.7 µm across the entire 1–50 Hz band. In a similar manner,

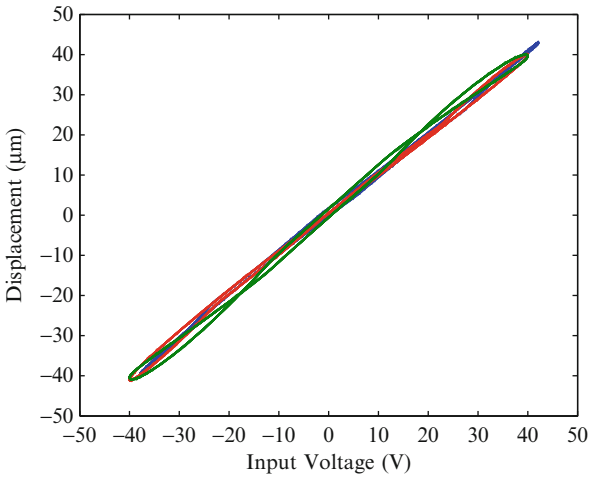

Fig. 9.4 Measured output displacement of the piezomicropositioning stage when the inverse rate-dependent Prandtl–Ishlinskii model is applied as a feed-forward compensator at different excitation frequencies between 1 and 50 Hz

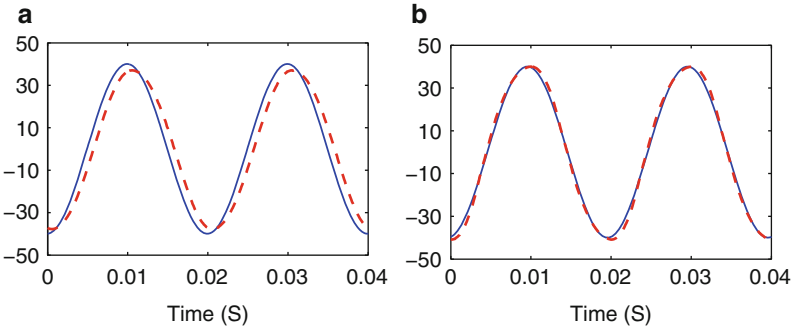

Fig. 9.5 The time history of the input voltage (*solid line*) and the measured displacement (*dashed line*) at excitation frequency of 50 Hz: (**a**) without the inverse compensator and (**b**) with the inverse compensator

Fig. 9.8 shows that the inverse compensator decreases the hysteresis percent to 3.5. It is obvious that the inverse rate-dependent Prandtl–Ishlinskii model suppresses the error due to rate-dependent hysteresis disregarding the excitation frequency of the input voltage and the tracking accuracy remains consistent.

In Fig. 9.18, the compensation effectiveness of the inverse rate-dependent Prandtl–Ishlinskii model is further evaluated by comparing the time history of the measured displacement responses of the piezomicropositioning stage with and without the inverse compensator at 20 and 50 Hz frequencies. The results show the effectiveness of the inverse rate-dependent model under low- and high-excitation frequencies.

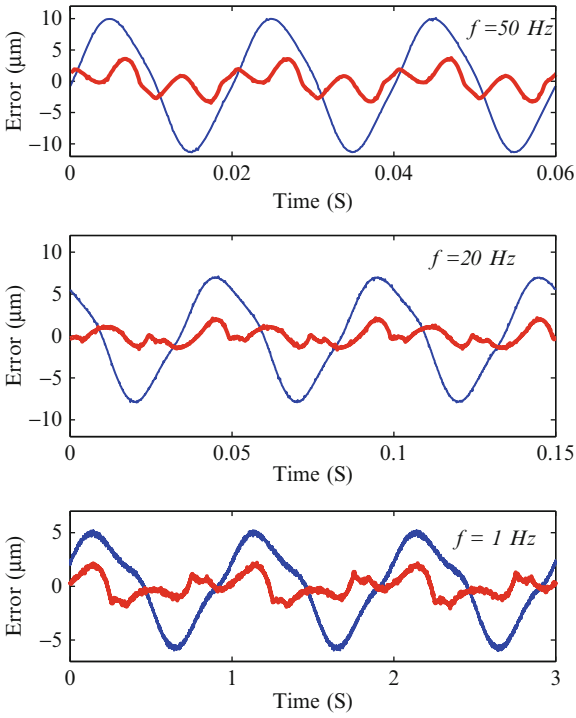

Fig. 9.6 Comparison of the positioning error with the inverse compensator (*red line*) and without the inverse compensator (*blue line*)

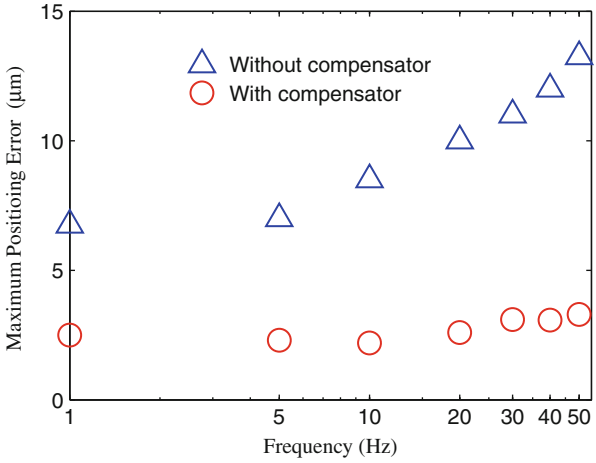

Fig. 9.7 Comparison between the maximum positioning error with and without inverse rate-dependent Prandtl–Ishlinskii model

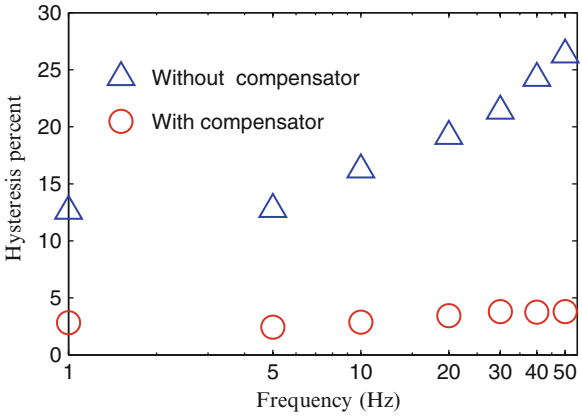

Fig. 9.8 Comparison between the percent of hysteresis nonlinearities with and without inverse rate-dependent Prandtl–Ishlinskii model

9.5.3 *Compensation of Hysteresis Nonlinearities at Low-Excitation Frequencies*

At low-excitation frequencies, the rate-dependent Prandtl–Ishlinskii model (9.3) and its inverse (9.9) constructed based on the dynamic threshold (9.20) are reduced to the rate-independent Prandtl–Ishlinskii model and its inverse. Analytically, the dynamic thresholds are reduced to

$$r(\dot{u}(t)) \approx \zeta i. \tag{9.28}$$

Then

$$\Pi[v](t) \approx \Psi[v](t). \tag{9.29}$$

Further investigation shows that the performance of the inverse rate-dependent Prandtl–Ishlinskii model still remains at low-excitation frequencies. In other words, the inverse rate-dependent Prandtl–Ishlinskii model can be applied to compensate for rate-independent hysteresis nonlinearities. As shown in Fig. 9.9, the inverse rate-dependent Prandtl–Ishlinskii model compensates for the hysteresis nonlinearities at excitation frequencies of 0.1 and 0.5 Hz. The time history for the positioning error is presented in Fig. 9.10. It can be concluded that the inverse rate-dependent Prandtl–Ishlinskii can be used as a feedforward compensator also at low-excitation frequencies.

9.5.4 *Triangular Waveform*

A triangular waveform of amplitude 40 at excitation frequencies of 10 and 20 Hz is applied as an input voltage. The experimental results show that the percent of the hysteresis nonlinearities are 13.54 and 15.62 for 10 Hz and 20 Hz, respectively. As shown in Fig. 9.11, the inverse model compensates for the hysteresis nonlinearities

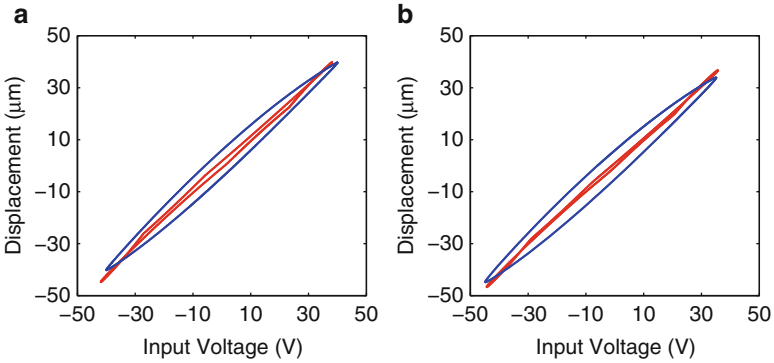

Fig. 9.9 The input–output of the piezomicropositioning actuator with (*red line*) and without (*blue line*) the inverse compensator at (**a**) $f = 0.10\,\text{Hz}$ and (**b**) $f = 0.50\,\text{Hz}$

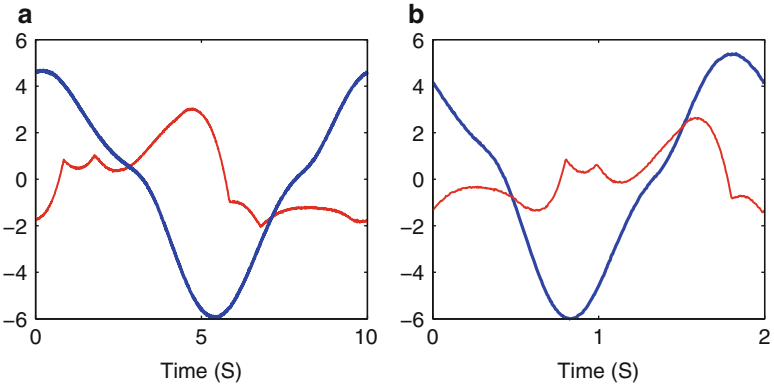

Fig. 9.10 The time history of the positioning error of the piezomicropositioning actuator with (*red line*) and without (*blue line*) the inverse compensator at (**a**) $f = 0.10\,\text{Hz}$ and (**b**) $f = 0.5\,\text{Hz}$

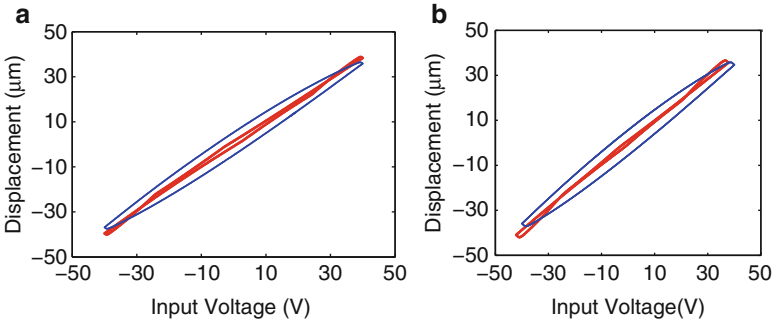

Fig. 9.11 The output of the piezomicropositioning stage with (*red line*) and without (*blue line*) the inverse compensator when a triangular waveform is applied at: (**a**) $f = 10\,\text{Hz}$ and (**b**) $f = 20\,\text{Hz}$

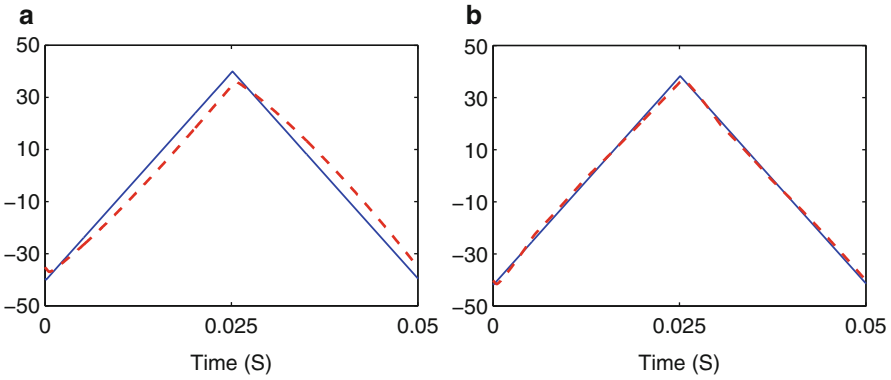

Fig. 9.12 The time history of the triangular input voltage (*blue line*) and the measured displacement (*red line*) at $f = 20\,\text{Hz}$: (**a**) without the inverse compensator and (**b**) with the inverse compensator

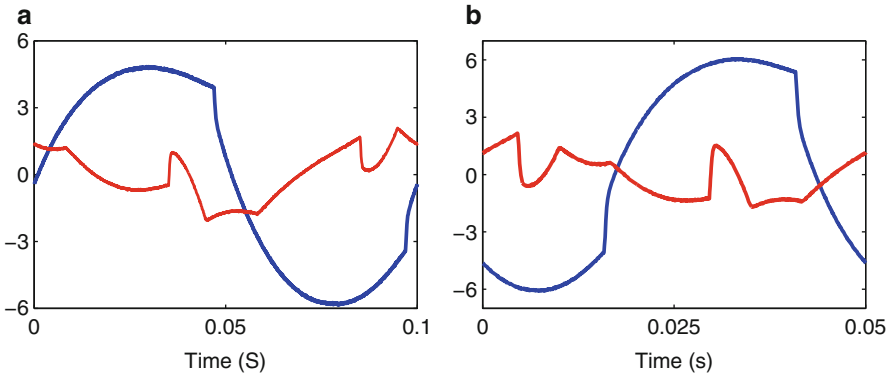

Fig. 9.13 The positioning error of Fig. 9.11 with (*red line*) and without (*blue line*) the inverse compensator: (**a**) $f = 10\,\text{Hz}$ and (**b**) $f = 20\,\text{Hz}$

when a triangular input voltage is applied. Figure 9.12 shows the triangular input voltage and the output displacement at the excitation frequency of 20 Hz with and without the inverse compensator. Figure 9.13 shows the time history of the positioning error with and without the inverse compensator. The results show the effectiveness of the inverse compensator when a triangular input voltage is applied at different excitation frequencies.

9.5.5 Major and Minor Hysteresis Loops

Major and minor hysteresis loops with the inverse rate-dependent Prandtl–Ishlinskii model are tested in this section (Fig. 9.14). Harmonic input voltages of $u(t) = 10\cos(2\pi ft) + 30\cos(4\pi ft)$ are applied to the piezomicropositioning actuator to

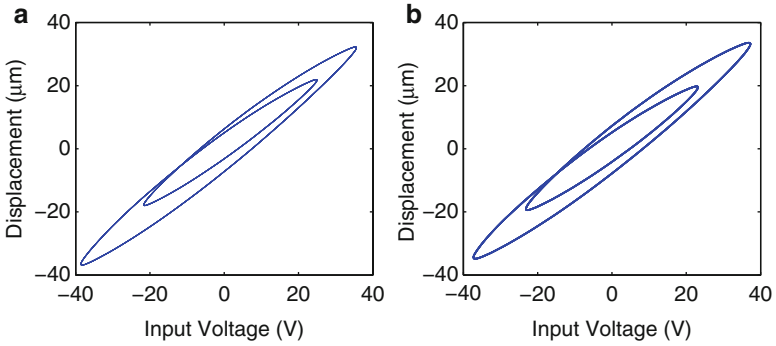

Fig. 9.14 The output of the piezomicropositioning actuator with the input voltage $u(t) = 10\cos(2\pi ft) + 30\cos(4\pi ft)$, where (**a**) $f = 5$ Hz and (**b**) $f = 10$ Hz

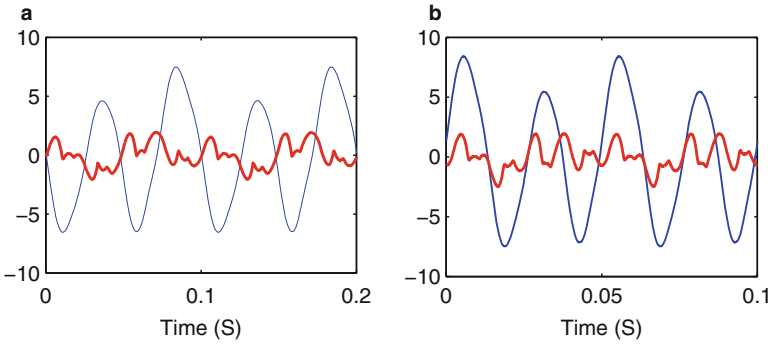

Fig. 9.15 The time history of the positioning error of Fig. 9.16 with the inverse compensator (*red line*) and without the inverse compensator (*blue line*) at: (**a**) $f = 5$ Hz and (**b**) $f = 10$ Hz

show major and minor hysteresis loops at excitation frequencies of $f = 5$ Hz and $f = 10$ Hz. Figure 9.15 shows the output of the inverse compensation. Figure 9.16 shows the time history of the positioning error with and without the inverse compensator.

9.6 Discussions

The above analysis shows that the inverse rate-dependent Prandtl–Ishlinskii model is capable of suppressing the error due to hysteresis, regardless of the excitation frequency of the input voltage, while maintaining consistency in the tracking accuracy (Fig. 9.17). The results manifest the effectiveness of the inverse rate-dependent model in compensating for hysteresis under low- and high-excitation frequencies. However, the inverse compensator shows some deviation in the output, which is attributed to prediction errors attained between the output of the rate-dependent model and the measured displacement of the piezomicropositioning

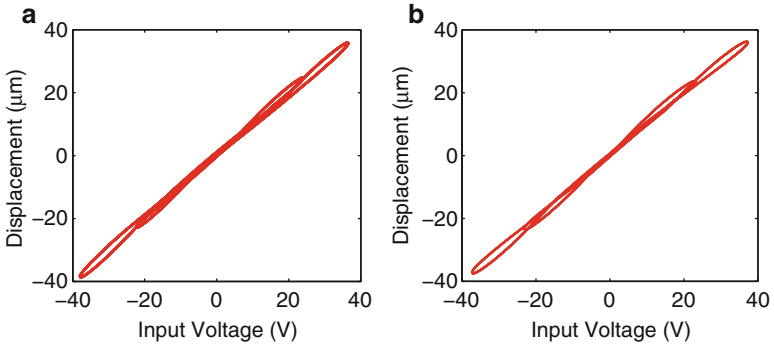

Fig. 9.16 The output of the piezomicropositioning actuator when the inverse rate-dependent Prandtl–Ishlinskii is applied as a feedforward compensator with the input voltage of $u(t) = 10\cos(2\pi ft) + 30\cos(4\pi ft)$, where (**a**) $f = 5$ Hz and (**b**) $f = 10$ Hz

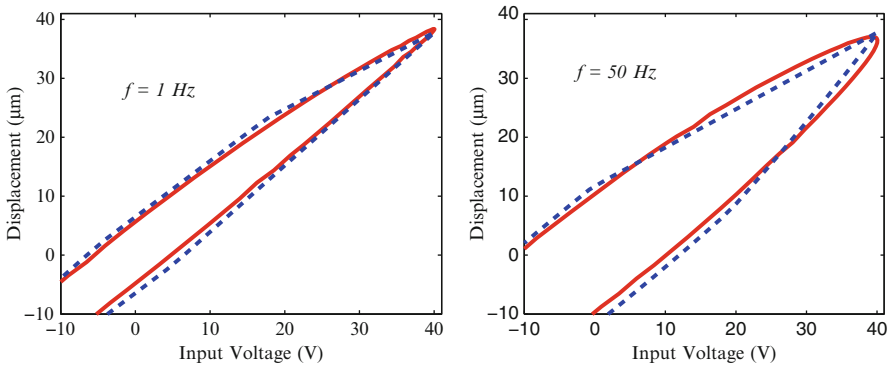

Fig. 9.17 Comparison between the measured displacement (*solid line*) and the output of the rate-dependent Prandtl–Ishlinskii model (*dashed line*) at excitation frequencies of 1 and 50 Hz

actuator. Figure 9.18 shows a comparison between the characterization error of the rate-dependent Prandtl–Ishlinskii model and the positioning error in the displacement output of the piezomicropositioning actuator. The figure shows a similarity between the error in both cases. It can be seen from the experimental results that the characterization error of the rate-dependent Prandtl–Ishlinskii model at the turning points is relatively larger than elsewhere. It should be mentioned that piezomicropositioning actuators also show creep effects during slow-speed actuation. These dynamic effects cause positioning errors in the output displacement.

As shown in the previous section, the inverse rate-dependent Prandtl–Ishlinskii model shows perfect compensation for symmetric hysteresis nonlinearities. However, the inverse model may not show the same performance when applied to compensate for asymmetric rate-dependent hysteresis nonlinearities. In future work, the inverse rate-dependent Prandtl–Ishlinskii model will be developed to compensate for asymmetric rate-dependent hysteresis nonlinearities of smart-material based actuators.

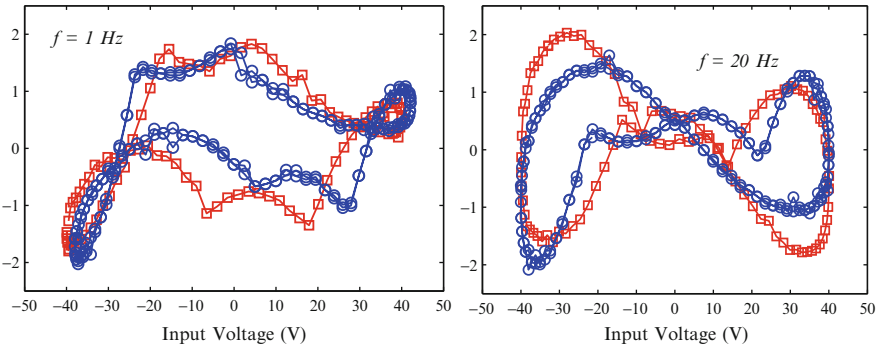

Fig. 9.18 Comparison between the error of the inverse compensation when the inverse rate-dependent Prandtl–Ishlinskii model is applied as a feedforward compensator (*circle*) and the characterization error between the measured displacement and the output of the rate-dependent Prandtl–Ishlinskii model (*square*)

It should be mentioned that different piezomicropositioning actuators exhibit asymmetric rate-dependent hysteresis nonlinearities that increase as the excitation frequencies of the applied input voltage increase. These effects can be accurately compensated for using the method proposed in this chapter. The results presented in this chapter can also be extended to complex hysteresis nonlinearities studied by Kuhnen [28] and Visone and Sjöström [29].

9.7 Conclusions

The inverse rate-dependent PrandtlIshlinskii model is analytical and exact. This makes the inverse PrandtlIshlinskii model attractive for control piezomicropositioning actuators at different excitation frequencies. The proposed compensation algorithm is easy to use and can be applied to compensate for rate-dependent hysteresis nonlinearities in micro/nano-positioning applications where the use of feedback sensors and feedback control techniques are not easy.

References

1. A. Cavallo, C. Natale, S. Pirozzi, C.Visone, A. Formisano, Feedback control systems for micropositioning tasks with hysteresis compensation. IEEE Trans. Magn. **40**(2), 876–879 (2004)
2. M. Rakotondrabe, C. Clevy, P. Lutz, Complete open loop control of hysteretic, creeped, and oscillating piezoelectric cantilevers. IEEE Trans. Autom. Sci. Eng. **7**(3), 440–450 (2010)
3. Y. Li, Q. Xu, A totally decoupled piezo-driven XYZ flexure parallel micropositioning stage for micro/nanomanipulation. IEEE Trans. Autom. Sci. Eng. **8**(2), 265–279 (2011)

4. D. Davinoa, C. Nataleb, S. Pirozzib, C. Visone, A phenomenological dynamic model of a magnetostrictive actuator. Physica B **343**(1–4), 112116 (2004)
5. B. Choi, M. Han, Vibration control of a rotating cantilevered beam using piezoactuators: experimental work. J. Sound Vib. **277**(1–2), 436–442 (2004)
6. B. Agrawal, M. Elshafei, G. Song, Adaptive antenna shape control using piezoelectric actuators. Acta Astronaut. **40**(11), 821–826 (1997)
7. P. Krejčí, M. Al Janaideh, F. Deasy, Inversion of hysteresis and creep operators. Physica B **407**(9), 1354–1356 (2012)
8. J. Park, K. Yoshida, S. Yokoto, Resonantly driven piezoelectric micropump-fabrication of a micropump having high power density. Mechatronics **9**(7), 687–702 (1999)
9. B. Mokaberi, A. Requicha, Compensation of scanner creep and hysteresis for AFM nanomanipulation. IEEE Trans. Autom. Sci. Eng. **5**(2), 197–206 (2008)
10. G. Tao, P. Kokotovic, Adaptive control of plants with unknown hysteresis. IEEE Trans. Automat. Contr. **40**(2), 200–212 (1995)
11. M. Al Janaideh, S. Rakheja, C.-Y. Su, Experimental characterization and modeling of rate-dependent hysteresis of a piezoceramic actuator. Mechatronics **17**(5), 656–670 (2009)
12. S. Viswamurthy, R. Ganguli, Modeling and compensation of piezoceramic actuator hysteresis for helicopter vibration control. Sensor Actuator A: Phys. **135**(2), 801–810 (2007)
13. R. Ben Mrad, H. Hu, A model for voltage-to-displacement dynamics in piezoceramic actuators subject to dynamic-voltage excitations. IEEE/ASME Trans. Mechatron. **7**(4), 479–489 (2002)
14. K. Leang, Q. Zou, S. Devasia, Feedforward control of piezoactuators in atomic force microscope systems: inversion-based compensation for dynamics and hysteresis. IEEE Contr. Syst. Mag. **19**(1), 70–82 (2009)
15. M. Grossard, M. Boukallel, N. Chaillet, C. Rotinat-Libersa, Modeling and robust control strategy for a control-optimized piezoelectric microgripper. IEEE/ASME Trans. Mechatron. **16**(4), 674–683 (2011)
16. P. Ge, M. Jouaneh, Tracking control of a piezoceramic actuator. IEEE Trans. Contr. Syst. Technol. **4**(3), 209–216 (1996)
17. H. Hu, H. Georgiou, R. BenMrad, Enhancement of tracking ability in piezoceramic actuators subject to dynamic excitation conditions. IEEE/ASME Trans. Mechatron. **10**(2), 230–240 (2005)
18. G. Song, J. Zhao, X. Zhou, J. Abreu-Garcia, Tracking control of a piezoceramic actuator with hysteresis compensation using inverse Preisach model. IEEE/ASME Trans. Mechatron. **10**(2), 198–209 (2005)
19. A. Esbrook, X. Tan, H. Khalil, Control of systems with hysteresis via servocompensation and its application to nanopositioning. IEEE Trans. Contr. Syst. Technol. 1–12 (2012). doi:10.1109/TCST.2012.2192734
20. Y. Shan, K. Leang, Repetitive control with Prandtl–Ishlinskii hysteresis inverse for piezo-based nanopositioning, in *Proceedings of the American Control Conference*, St. Louis, MO, 2009, pp. 301–306
21. W. Ang, P. Khosla, C. Riviere, Feedforward controller with inverse rate-dependent model for piezoelectric actuators in trajectory-tracking applications. IEEE/ASME Trans. Mechatron. **12**(2), 134–142 (2007)
22. M. Al Janaideh, P. Krejčí, An inversion formula for a Prandtl–Ishlinskii operator with time dependent thresholds. Physica B **406**(8), 1528–1532 (2011)
23. P. Krejci, K. Kuhnen, Inverse control of systems with hysteresis and creep. IEE Proc. Contr. Theor. Appl. **148**(3), 185–192 (2001)
24. A. Bergqvist, On magnetic hysteresis modeling, Ph.D. thesis, Royal Institute of Technology, Stockholm, Sweden, 1994
25. P. Krejčí, Hysteresis and periodic solutions of semilinear and quasilinear wave equations. Math. Z. **193**, 247–264 (1986)
26. M. Brokate, J. Sprekels, *Hysteresis and Phase Transitions* (Springer, New York, 1996)

27. K. Kuhnen, P. Krejčí, Compensation of complex hysteresis and creep effects in piezoelectrically actuated systems: a new preisach modeling approach. IEEE Trans. Automat. Contr. **54**(3), 537–550 (2009)
28. K. Kuhnen, Modeling, identification and compensation of complex hysteretic nonlinearities—a modified Prandtl–Ishlinskii approach. Eur. J. Contr. **9**(4), 407–418 (2003)
29. C. Visone, M. Sjöström, Exact invertible hysteresis models based on play operators. Physica B **343**(1–4), 148–152 (2004)